

High-Mannose Glycans are Elevated during Breast Cancer Progression*[§]

Maria Lorna A. de Leoz‡, Lawrence J. T. Young§, Hyun Joo An‡, Scott R. Kronewitter‡, Jaehan Kim¶, Suzanne Miyamoto||, Alexander D. Borowsky§, Helen K. Chew||, and Carlito B. Lebrilla‡**‡‡

Alteration in glycosylation has been observed in cancer. However, monitoring glycosylation changes during breast cancer progression is difficult in humans. In this study, we used a well-characterized transplantable breast tumor mouse model, the mouse mammary tumor virus-polyoma middle T antigen, to observe early changes in glycosylation. We have previously used the said mouse model to look at O-linked glycosylation changes with breast cancer. In this glycan biomarker discovery study, we examined N-linked glycan variations during breast cancer progression of the mouse model but this time doubling the number of mice and blood draw points. N-glycans from total mouse serum glycoproteins were profiled using matrix-assisted laser desorption/ionization Fourier transform-ion cyclotron resonance mass spectrometry at the onset, progression, and removal of mammary tumors. We observed four N-linked glycans, *m/z* 1339.480 (Hex₃HexNAc), 1485.530 (Hex₃HexNAc₄Fuc), 1809.639 (Hex₅HexNAc₄Fuc), and 1905.630 (Man₉), change in intensity in the cancer group but not in the control group. In a separate study, N-glycans from total human serum glycoproteins of breast cancer patients and controls were also profiled. Analysis of human sera using an internal standard showed the alteration of the low-abundant high-mannose glycans, *m/z* 1419.475, 1581.528, 1743.581, 1905.634 (Man₆₋₉), in breast cancer patients. A key observation was the elevation of a high-mannose type glycan containing nine mannoses, Man₉, *m/z* 1905.630 in both mouse and human sera in the presence of breast cancer, suggesting an incompleteness of the glycosylation process that normally trims back Man₉ to produce complex and hybrid type oligosaccharides. *Molecular & Cellular Proteomics* 10: 10.1074/mcp.M110.002717, 1–9, 2011.

Breast cancer is the leading cause of cancer death and the most frequently diagnosed cancer among women worldwide

From the ‡Department of Chemistry; §Center for Comparative Medicine; ¶Department of Viticulture and Enology; and **Department of Biochemistry, University of California Davis, Davis, CA 95616; and ||Clinical Breast Cancer Program, University of California Davis Cancer Center, Sacramento, CA 95817

Received July 6, 2010, and in revised form, November 15, 2010
Published, MCP Papers in Press, November 19, 2010, DOI 10.1074/mcp.M110.002717

(1). In the United States alone, ~40,000 deaths and 210,000 new cases were expected in 2010 (2). Incidence rates continue to rise especially in many developing and westernized countries. Unfortunately, early stages of breast cancer show no noticeable symptoms. Early diagnosis is critical because the chance of survival is greater in early stage (Stage I and II) breast cancer. It is estimated that 98% of U. S. women will survive longer than 5 years if the cancer is detected early. At late stages (Stages III and IV), however, only 28% will survive longer than 5 years (1).

Currently, carbohydrate antigen 15-3 (CA 15-3) is the most common clinical serum marker for breast cancer. This marker uses immunoassay to detect MUC-1, a mucin glycoprotein overexpressed with breast cancer. Other markers for breast cancer include carcinoembryonic antigen, an anchored glycoprotein involved in cell adhesion, and CA 27.29, another MUC-1-derived glycoprotein marker. A common feature of these three markers is that all are proteins containing glycoforms.

However, the current markers described above are not recommended by the American Society of Clinical Oncology as markers for screening, diagnostic, or staging tests for breast cancer (3). During the early stages of breast cancer, the sensitivity (*i.e.* patients correctly identified) of these markers is less than 25% (3–7). Moreover, the specificity (*i.e.* people without cancer correctly identified) is also problematic: up to 20%–30% of women without breast cancer, *i.e.* healthy individuals, women with benign breast lesions, people with benign diseases such as liver disease, and people with other types of advanced adenocarcinoma, have elevated levels of the said markers (3–7). Thus, an elevated marker level is not specific to breast cancer and may lead to false positive diagnoses for the healthy individual.

Aberrant glycosylation is observed in the progression of many types of diseases, including different cancers (8, 9). Glycosylation, one of the most common forms of post-translational modification, is highly sensitive to the biochemical environment. Thus, instead of looking at the proteins to which these glycans are attached, a new paradigm is to look at the commonly disregarded oligosaccharides and find their correlation with cancer. For example, Rudd and coworkers (10) analyzed fluorescently tagged serum N-glycans of advanced breast cancer patients using exoglycosidases and high-per-

formance liquid chromatography coupled to matrix-assisted laser desorption/ionization time-of-flight mass spectrometry (MALDI-TOF MS)¹ and found that specific glycans were changing during breast cancer progression. Specifically, they found a trisialylated triantennary glycan containing an α -1,3-linked fucose as increasing in the presence of breast cancer.

Novotny and coworkers profiled the permethylated *N*-glycans in sera of breast cancer patients at different stages (stages I to IV) using MALDI TOF/TOF MS in one study (11) and profiled reduced and methylated serum *N*-glycans of late-stage breast cancer patients using nano-liquid chromatography (LC) Chip/time-of-flight (TOF) MS in another study (12). In both studies, they found an increase in fucosylation in both core and branched segments of *N*-glycans in the presence of breast cancer, which may be because of the elevation of sialyl Lewis^x in cancer. In the latter study, they found a decrease in intensity in a biantennary-monosialylated *N*-linked glycan and an elevation in a fucosylated triantennary-trisialylated *N*-linked glycan in the presence of Stage IV breast cancer.

Our review on glycan disease markers (13) summarized specific glycan changes observed with different types of cancer such as degree of branching and number of sialic acid, fucose, and mannose residues. These glycosylation changes are known to correlate with tumor growth, adhesion, metastasis, and immune surveillance of tumor. We deem that monitoring glycans during cancer progression may give more specific and sensitive cancer markers.

However, monitoring glycosylation changes at the onset of and during breast cancer progression is difficult in humans. We have previously used the Polyoma Middle-T transplantable mouse breast cancer tumor model to monitor the *O*-linked glycans, *i.e.* glycans attached to the serine (Ser) or threonine (Thr) residue of the glycoprotein, in mouse sera (14). This metastatic breast cancer model was generated from inbred mice transgenic for the Polyomavirus middle-T gene (15) that were transplanted with Met-1 metastatic breast cancer tumors. The histopathology of Polyomavirus middle-T hyperplasia has been comprehensively characterized and transplantation experiments for these have been established (15–17). The *O*-linked glycans were released by β -elimination and analyzed by MALDI Fourier transform ion cyclotron resonance (FT-ICR) MS and infrared multiphoton dissociation (IRMPD). We have also looked at *N*-linked glycans, *i.e.* glycans with a common trimannosyl chitobiose core attached to asparagine (Asn) occurring in the sequon Asn-X-Ser/Thr, where X could be any amino acid except proline (Pro), as potential bi-

omarkers for prostate cancer (18). These *N*-linked glycans were released with peptide *N*-glycosidase F (PNGase F).

In this glycan biomarker exploratory study, we monitored the *N*-linked glycans in a bigger sample set of the PyMT mouse model using MALDI FT-ICR MS, an MS technique that we have proven to be useful in the given complex biological sample (19). And in parallel, we did a small cohort of human sera to show our method of looking at high-mannose glycans using internal standards.

Mass spectrometry (MS) of glycans has led to several potentially promising markers for several diseases (14, 18, 20–24). The *N*-linked glycan compositions and putative structures were assigned based on the accurate mass values obtained from the FT-ICR mass spectrometer and sound knowledge in glycobiology. Compared with the other mass spectrometric techniques, FT-ICR still provides the best performance with its exceptional mass accuracy at few parts per million (ppm) error and extremely high mass resolution. It has been used extensively and successfully in complex samples. We have shown in our previous studies how FT-ICR MS, with proper deconvolution to monoisotopic masses, can radically improve the compositional assignments of glycans (19, 25). Further confirmation of structures of the most abundant species was done using Sustained off-resonance irradiation collision-induced dissociation (SORI-CID) and IRMPD MS/MS in conjunction with the MALDI FT-ICR MS.

Although the mouse model does not fully resemble the human model, it gives us insight into how serum glycan intensities change during the tumor's progression because transplantation and removal of tumors can be done at defined time points. For comparison, glycan profiles of sera from women with highly metastatic breast cancer and healthy women with no history of cancer were also profiled.

EXPERIMENTAL PROCEDURES

Mouse Serum Samples—Sera were collected via orbital eye bleeding of female inbred FVB mice ($n = 8$). Blood was drawn from week 0 till week 10 every 2 weeks. There were cases where it was not possible to obtain blood samples. Therefore, three mice had only five instead of six blood samples. Samples were frozen at 80 °C until processing. The cancer group ($n = 4$) consisted of mice surgically transplanted with 1 mm³ pieces of highly metastatic breast tumors, polyoma middle-T Met-1, at week 0. Tumors were removed at week 4. The control group ($n = 4$) included two mice without surgery and two mice surgically opened at weeks 0 and 4 but with no tumor transplanted. Mice were sacrificed at week 10.

Human Serum Samples—Twelve serum samples from women with highly metastatic breast cancer ($n = 7$, collectively called cancer group) and healthy women with no known history of cancer ($n = 5$, control group) were acquired from the University of California-Davis Medical Center Clinical Laboratories using an IRB-approved protocol. Informed consent was obtained from all subjects. Serum samples were collected by standard venous phlebotomy, stored in standard clot tubes and frozen at –80 °C before processing.

Enzymatic Release of *N*-linked Glycans—*N*-linked glycans were released using our established procedures (18, 19). Briefly, 50–100 μ l of human or mouse serum was added to 100 μ l of digestion buffer consisting of 200 mM ammonium bicarbonate (NH₄HCO₃, Sigma-

¹ The abbreviations used are: MALDI FT-ICR MS, matrix-assisted laser desorption/ionization Fourier transform-ioncyclotron resonance mass spectrometry; IRMPD - infrared multiphoton dissociation; PNGase F - peptide *N*-glycosidase F; MMTV-PyMT - mouse mammary tumor virus-polyoma middle T antigen; HPLC, high-performance liquid chromatography; ACN, acetonitrile.

Aldrich, St. Louis, MO) and 10 mM dithiothreitol (Promega, Madison, WI). The mixture was heated to 100 °C to denature the proteins. Following cooling to room temperature, 2.5 μ l of peptide *N*-glycosidase F (PNGase F) (500,000 units/ml, New England Biolabs, Ipswich, MA) was added and the mixture was incubated either at 37 °C for 24 h in a water bath or at 37 °C for 10 min using a microwave reactor. Eight-hundred microliters of chilled ethanol (Gold Shield, Hayward, CA) was added. The mixture was frozen to –80 °C for 1 h and then centrifuged for 20 min at 13,200 rpm. The supernatant was decanted and evaporated to dryness using a vacuum centrifugal evaporator (Savant AES 2010).

Glycan Purification by Graphitized Carbon-Solid Phase Extraction—The recovered supernatant was purified and fractionated by solid phase extraction using a graphitized carbon cartridge with 150 mg bed weight and 4-ml cartridge volume (Grace Davison, Deerfield, IL). The cartridge was conditioned with nanopure water and 80% acetonitrile (ACN) in 0.05% aqueous trifluoroacetic acid (v/v). The glycan solution was loaded onto the cartridge and desalted with nanopure water (12 ml) at a flow rate of about 1 ml/min. Glycans were eluted with aqueous 10% ACN, 20% ACN, and 40% ACN with 0.05% trifluoroacetic acid (v/v). Each fraction was collected and dried in a centrifugal evaporator and reconstituted in nanopure water prior to mass spectrometry analysis.

Mass Spectrometric Analysis

MALDI FT-ICR MS and MS/MS Analysis—Mass spectra were recorded on an FT-ICR MS with an external source ProMALDI (Varian, Palo Alto, CA) equipped with a 7.0 Tesla magnet. The ProMALDI was equipped with a pulsed Nd:YAG laser operating at 355 nm. Internal calibration was done using pre-identified serum glycan peaks, allowing mass accuracy of 10ppm or better. 2,5-Dihydroxy-benzoic acid was used as a matrix (5 mg/100 μ l in 50% ACN:H₂O) for both positive and negative modes. Sodium chloride (NaCl) (0.01 M in 50% ACN:H₂O) was used as a cation dopant for the positive ion mode. Thus, the *N*-linked glycans were seen either as [M+Na]⁺ or [M-H][–] in the positive or negative ion modes, respectively. Three spectral acquisitions, each with 10 laser shots, were acquired on the 10%, 20%, and 40% aqueous ACN fractions of a sample, giving a total of nine spectra per time point (for mouse sera) or per sample (for human sera). Tandem mass spectrometry using collision-induced dissociation (CID) and infrared multiphoton dissociation (IRMPD) was performed to confirm *N*-linked glycan compositions.

High Performance Liquid Chromatography (HPLC) Chip/Time-of-Flight (TOF)-MS Analysis—Glycan fractions were analyzed using an Agilent 6200 Series HPLC Chip/TOF-MS system as described previously (26). Briefly, separation was performed using a binary gradient solvent system consisting of A: 3% ACN in 0.1% formic acid solution, and B: 90% ACN in 0.1% formic acid solution. The column was initially equilibrated and eluted at a flow rate of 0.4 μ l for nanopump and 4 μ l for capillary pump. The gradient ran for 65 min and was programmed as follows: 2.5–20min: 0%–16% B; 20–30 min: 16%–44%B; 30–35min: B increased to 100%; 35–45 min: continue at 100% B; and 45–65 min: 0% B to equilibrate the chip column before next sample injection. Glycan compositions were determined using Glyco X (27) based on masses and retention times.

Quantification using an Internal Standard—To quantify *N*-linked glycans in the human sera, maltohexose ([M+Na]⁺, *m/z* 1013.3167) was used as an internal standard. Samples were doped with a fixed amount of maltohexose and their mass spectral intensities were surveyed for possible neutral (mannose, fucose, and complex-type) and acidic (sialic acid) oligosaccharide masses relative to maltohexose. The intensities of the glycans were then scaled to the intensities of maltohexose to yield a corrected intensity.

Data Analysis—Mass spectra were acquired and calibrated using IonSpec Omega version 8.0 (Varian). Calibration was done internally with less than 5 ppm mass error. Oligosaccharides were identified in the first pass using an in-house program called Glycan Finder written in Igor Pro version 5.04B (Wavemetrics) using exact masses with a tolerance of 10 ppm. Then, a biological filter was applied following Cooper's method as explained in our previous work (26). One-way analysis of variance of the glycan intensities was then performed to compare between time points and groups. A *p* value less than 0.05 is considered a significant difference. The Dixon's Q-test was used to determine outliers.

RESULTS

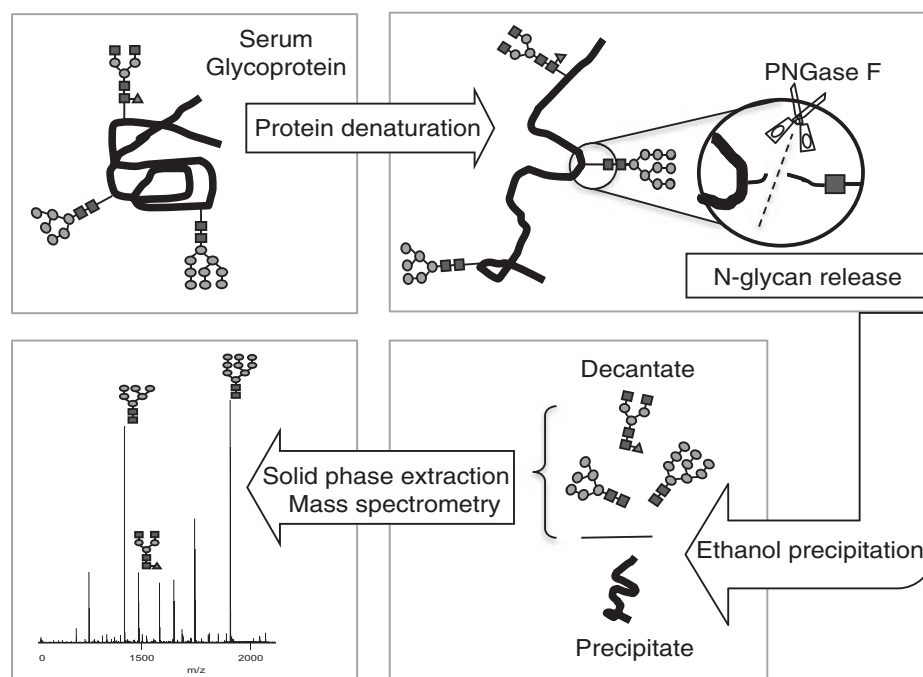
***N*-linked Glycans During Breast Tumor Progression in Mouse Sera**—The workflow of analysis is outlined in Fig. 1. *N*-linked glycans from denatured serum glycoproteins of a) mouse sera collected pre- and postbreast tumor implantation, and b) sera of women with and without breast cancer were globally released using the enzyme Peptide *N*-glycosidase F. Cold ethanol is subsequently added to precipitate the proteins out of the solution (28). Glycans remaining in the supernatant were then desalted, purified, and partitioned into neutral and acidic glycans by graphitized carbon solid phase extraction with the eluants profiled by MALDI FT-ICR MS.

Glycan profiles during breast tumor progression in mice show intensity variations in some glycans. Week 0 was designated as the baseline and Week 4 was the tumor point, because the tumor was removed following blood extraction at Week 4. Fig. 2A shows the mass spectral profile of serum *N*-linked glycans of a tumor-transplanted mouse at Week 4. A total of 68 *N*-linked glycan compositions were found from the three ACN fractions across eight mouse serum samples using MALDI FT-ICR MS. More than 150 glycans were found in mouse sera using the HPLC Chip/TOF MS (See Supplemental Tables 1–3). Perreault and coworkers (29) provided a comprehensive list of glycans in CD-1 nude mouse serum with and without head and neck tumor. Most of the glycans they reported were also seen in our mouse glycan profile, although we have fractionated our samples into 10%, 20%, and 40% acetonitrile fractions, the neutral ones eluting at 10% and 20% and the acidic at 40%, in order to see as much of the low-abundant glycans as possible.

We observed that the abundant glycans in the 10% ACN fraction spectra taken in the positive ion mode were mainly the high-mannose *N*-linked glycans (Man_{5–9}GlcNAc₂) and complex biantennary glycans. These glycans varied in intensity over the course of tumor progression but were always observed in the spectra. A total of 33 glycan compositions were seen in the 10% ACN fraction using MALDI FT-ICR MS.

In the 20% ACN fraction spectra taken in the positive ion mode, the abundant peaks were neutral complex-type glycans. Forty-three glycan compositions were observed in the 20% ACN fraction, but 20 of these were also found in the 10% ACN fraction. Thus, only 23 compositions were unique to the 20% ACN fraction. The high-mannose glycans were still in the spectra but it is of much lower intensity than the complex glycans.

FIG. 1. Strategy used in the analysis of N-linked glycans in the serum samples. N-linked glycans were released from denatured glycoproteins in the serum by PNGase F enzymatic digestion. Ethanol was added to precipitate the proteins, leaving the glycans in the supernatant. Fractionation and purification was done by solid phase extraction using graphitized carbon cartridges. Mass spectra were recorded on a MALDI FT-ICR MS. Symbol representations of glycans (39): N-acetylglucosamine, black square; mannose, gray circle; galactose, white circle; fucose, dark gray triangle; N-acetylneuraminic acid, dark gray diamond.



The 40% ACN fraction spectra taken in the negative ion mode contained mostly sialylated N-linked glycans, *i.e.* glycans containing N-glycolyl neuraminic acid (NeuGc) residues. Fourteen (14) glycan compositions were seen in this fraction with two (2) glycan peaks found in all three fractions. Thus, only 12 were found solely in the 40% ACN fraction.

The two glycan compositions that were found present in all fractions, m/z 1785.64 and 1988.72, correspond to neutral complex fucosylated glycans that differ by one N-acetylhexosamine (HexNAc) ($\text{Hex}_5\text{HexNAc}_4\text{Fuc}$ and $\text{Hex}_5\text{HexNAc}_5\text{Fuc}$, respectively). These glycans were observed as $[\text{M}-\text{H}]^-$ in the negative mode. Although it is sometimes possible to see neutral glycans in the negative ion mode, we cannot rule out the possibility that this glycan may come from sialylated species with the sialic acid lost during analysis. Fucose is another labile monosaccharide that apparently remains intact during the ionization conditions employed in this study. Although fragmentation during the ionization process can never be eliminated, we minimize its effects by performing the analysis under identical conditions.

Serum N-linked Glycan Profile of Women with Metastasized Breast Cancer—The N-linked glycan profile of human sera is shown in Fig. 2B. The abundant peaks in the 10% ACN fraction spectra taken in the positive ion mode of MALDI are primarily neutral fucosylated complex-type glycans. The high-mannose glycans are present in the 10% ACN fraction but not abundantly. This feature is the most distinctive between mouse and human sera in that mouse sera have significant more high mannose species than human.

The 20% ACN fraction spectra of the human sera taken in the positive mode contain the neutral complex glycans as the abundant species. They are, however, of higher m/z than in

the 10% ACN fraction. The 40% ACN fraction spectra in the negative ion mode show the acidic glycans as the abundant glycans. In Fig. 2, only the abundant peaks were annotated in both human and mouse sera. However, there are many more low-abundant peaks observed upon zooming in on the spectra. Approximately 100 glycan compositions were observed in the human sera.

Distinct Differences in N-linked Glycan Intensities Between Cancer and Control in Mouse and Human Sera—Fig. 3 shows the m/z 1000–2000 region of the 10% ACN fraction of a representative A) control (mock surgery) and B) tumor-transplanted mouse serum glycans from Week 0 to Week 10. This region contains most of the glycans in the 10% ACN fraction. The glycan intensity can be seen varying during tumor transplantation and removal. For example, in Fig. 3B, Man_9 (m/z 1905.630) has a relative intensity of around 45% before the tumor was transplanted, and the intensity stays elevated to 100% whereas the tumor is there. At Week 6, the intensity falls down to 60%, and stays at less than 30% until the mouse is sacrificed at Week 10. In Fig. 3A, Man_9 remains below 40% in intensity throughout Week 0 to Week 10. Another glycan with m/z 1485.530 ($\text{Hex}_3\text{HexNAc}_4\text{Fuc}$) starts at a relative intensity of around 85% before transplantation in Fig. 3B and plummets to less than 20% whereas the tumor is present and then the intensity goes up again and stays elevated at around 90% after the tumor was removed. This same glycan remained high in all six time points in Fig. 3A.

Fig. 4 shows the trends in changes in intensity of high-mannose glycans during the course of experiment in representative mice. Changes in high-mannose glycans were not considerably significant throughout the course of the experiment in the control mice, both in the intact and mock-surgery

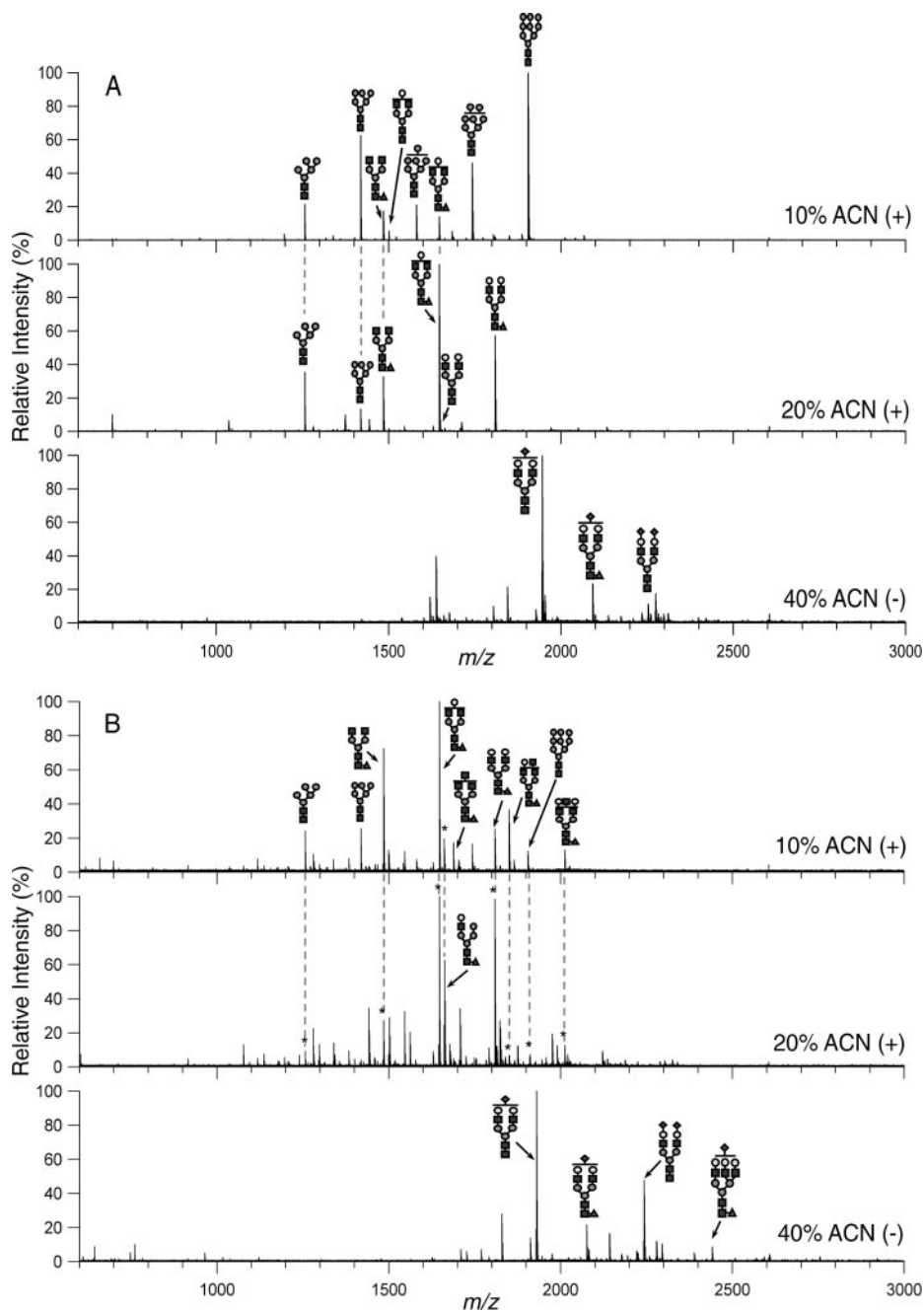


FIG. 2. MALDI FT-ICR MS representative profiles of *N*-linked glycans in mouse and human sera from the 10%, 20%, and 40% acetonitrile (ACN) fractions taken in positive (10% and 20%) and negative (40%) ion modes. Profiles shown are from (A) serum of a tumor-transplanted mouse in its 2nd week and (B) serum of a human with breast cancer. Only the abundant *N*-linked glycans were annotated. Structures are putative and based on exact mass and when possible, MS/MS. An * indicates that the peak is identical in mass and already annotated in the previous fraction. See Fig. 1 for glycan symbols.

groups. In cancer mice, however, there was an increase in intensities of at least two species (Man_8 and Man_9) from Week 0 (baseline) to Week 4 (tumor), and abrupt decrease in intensities after the tumor was removed. The intensity drop persisted until the mice were sacrificed at Week 10. This is especially true for Man_9 . Intensity of Man_9 went from less than 20% at Week 0 to around 80% at Week 4, then to around 10%–20% thereafter.

Interestingly, two abundant monofucosylated biantennary complex glycans, m/z 1485.530 ($\text{Hex}_3\text{HexNAc}_4\text{Fuc}$) and m/z 1647.587 ($\text{Hex}_4\text{HexNAc}_4\text{Fuc}$), had noticeable drop in intensity

from Week 0 to Week 4 in the cancer mice that rose again once the tumor was removed. Following Week 4, however, these same glycans showed a general increase in intensity over time for both the control and cancer mice. This leads us to believe that fucosylation might be related to aging. Vanhooren *et al.* (30, 31) showed this same glycan as gradually increasing with aging in their study of 100 human sera.

Four *N*-linked glycan peaks were identified as changing significantly (p value < 0.05) between the pre-tumor and tumor time points in the cancer group, as shown in Fig. 5: m/z 1339.480 ($\text{Hex}_3\text{HexNAc}_4$), m/z 1485.530 ($\text{Hex}_3\text{HexNAc}_4\text{Fuc}$),

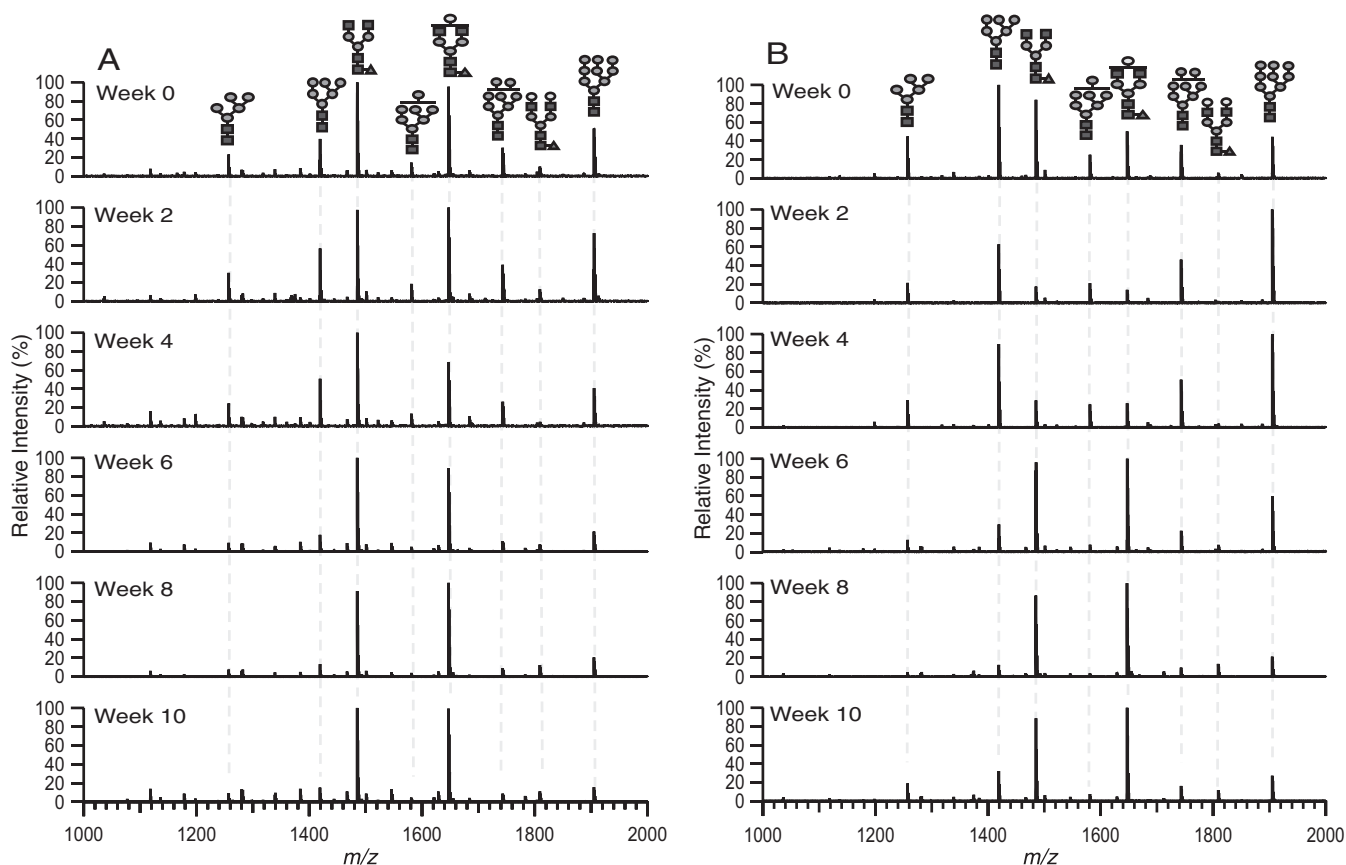


FIG. 3. Representative MALDI FT-ICR mass spectra of **A**, mock surgery control and **B**, tumor-transplanted mouse sera at different time points. m/z 1000–2000 region of 10% acetonitrile fraction taken in the positive ion mode is shown. See Fig. 1 for glycan symbols.

m/z 1809.639 ($\text{Hex}_5\text{HexNAc}_4\text{Fuc}$), and m/z 1905.630 ($\text{Hex}_9\text{HexNAc}_2$). Glycans with m/z 1339.480 and m/z 1485.530 were decreasing in intensity with cancer whereas m/z 1809.639 and m/z 1905.630 were elevated with cancer. No significant changes in these four N -linked glycans were observed in the two controls.

Figs. 5 and 6 show a summary of glycans that significantly vary in the cancer and control groups for both mouse and human sera, respectively. Although the N -linked glycan profiles of human sera are different from mouse sera, the high-mannose type N -linked glycans were elevated with cancer in both cases. In addition, one high-mannose type glycan Man_9 , m/z 1905.630, was found to increase significantly with cancer for both human and mouse sera.

DISCUSSION

N -linked glycans have been shown to change in the presence of cancer. Thus, we monitored the N -linked glycans during the progression of breast cancer in mice. N -linked glycans globally released from mouse sera collected pre- and post-breast tumor implantation, and sera of women with and without breast cancer were all profiled using MALDI FT-ICR MS.

Sera of cancer-transplanted mice were compared against two control groups; intact group and mock-surgery group.

The two control groups were necessary to determine whether glycan changes were a result of stress or trauma from the surgery. Specific glycans were identified as changing significantly in the cancer-transplanted mice before and after tumor transplantation but not changing significantly in both the intact and mock-surgery mice.

As a separate study, serum glycan profiles of women with breast cancer were also acquired. Women with highly metastatic breast cancer were compared with healthy women with no history of cancer. This sample set gave the greatest degree of separation between cancer and control. We had to quantitate with an internal standard because the intensities for the glycans we wanted to monitor, *i.e.* high mannose glycans, were not high. The quantitation method used for human sera was unnecessary for the mouse sera as the intensities were high. We found that the separation between control and cancer groups for human was greatest for the high-mannose glycans. The presence of a glycan having 10 hexoses was noted and designated as Man_9+Hex because this species might have arisen from an uncleaved glucose early in the N -linked glycan biosynthetic pathway.

Although we saw two fucosylated glycans as changing in glycoproteins in mouse sera in the presence of cancer as shown in Fig. 5, we focused mainly on the high-mannose glycans'

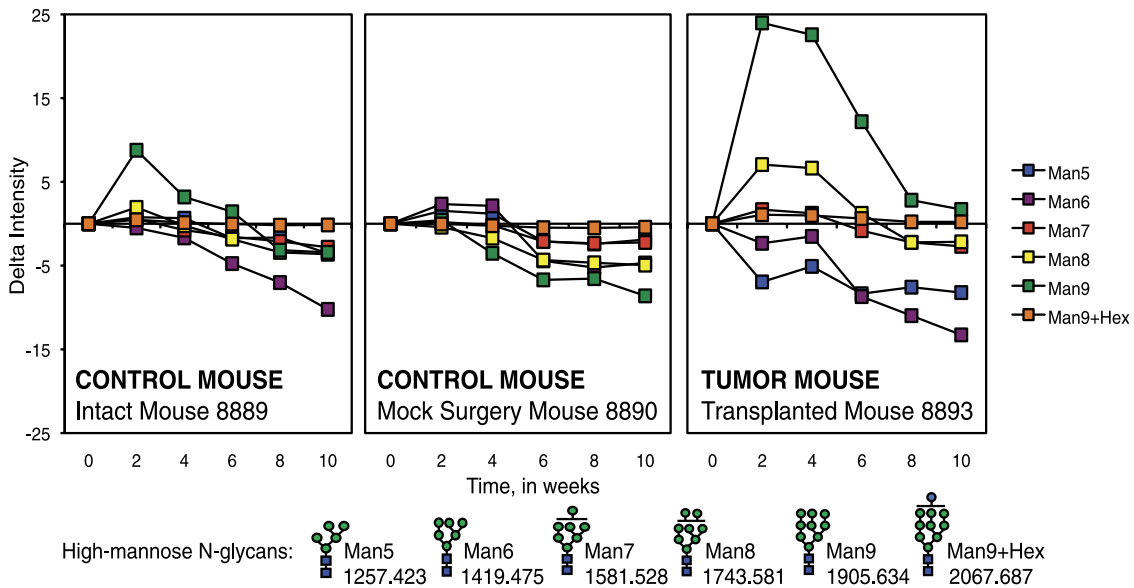


FIG. 4. Change in intensities from MALDI FT-ICR MS of high-mannose *N*-linked glycans in sera of an intact control mouse, mock surgery control mouse, and a tumor-transplanted mouse during breast cancer progression. All values relative to Week 0 intensity. Error bars are expressed as standard error of the mean (S.E.) from three spectral scans per mouse sample. Symbol representations of glycans (39): *N*-acetylglucosamine, blue square; mannose, green circle; glucose, blue circle.

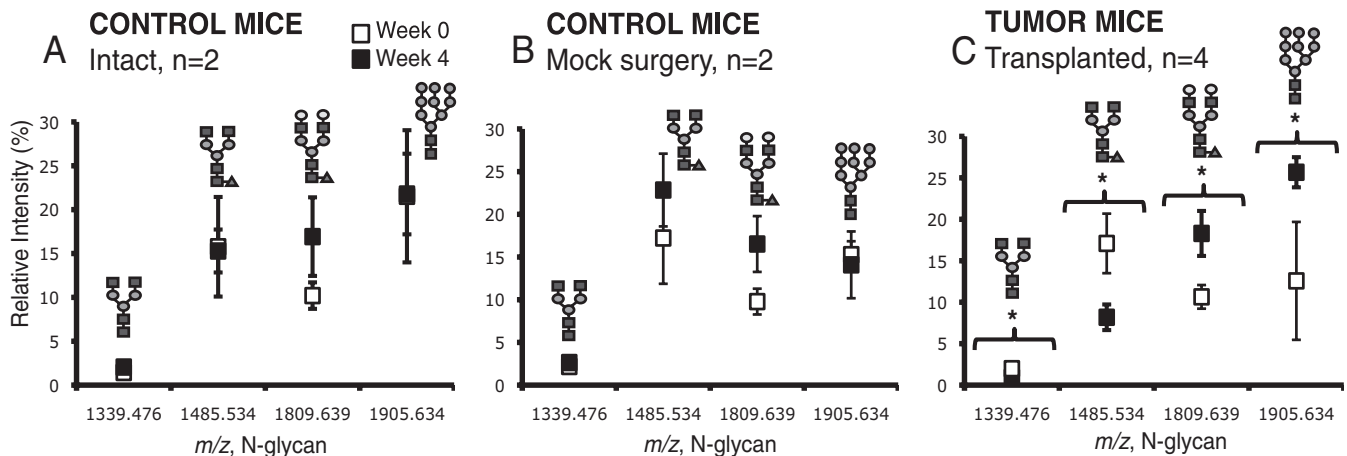


FIG. 5. *N*-linked glycans that are statistically different at Week 0 (pretumor) and Week 4 (tumor) in mouse sera of tumor-transplanted mice (C). These same glycans are not statistically different at Week 0 and 4 in mouse sera of both the intact (A) and mock surgery (B) control mice. All glycans except *m/z* 1809.639 are from the 10% ACN fraction. Glycan *m/z* 1809.639 is from the 20% ACN fraction. Glycans marked with * have *p* value < 0.05. Glycans were analyzed using MALDI FT-ICR MS. Error bars are expressed as S.E. See Fig. 1 for glycan symbols.

elevation and looked at it closely in human sera. The potential markers, especially the sialylated and fucosylated glycans seen by Rudd (10) and Novotny (11, 12), was not seen as changing significantly in our current study but is part of our future studies.

The abundance of high mannose glycans, specifically Man₉ correlates well with the progression of cancer. When the tumor burden is increased, the intensity of Man₉ increases, and when the tumor is removed, the intensity of Man₉ decreases. Man₉, interestingly, was observed to be elevated in both mouse and human serum sample sets.

The elevation of high mannose glycans is consistent with other reports that correlate their behavior with cancer. For example, Man₅-Man₇ glycans were present in mice implanted

with head and neck tumor but not in healthy mice (29). In a different study, Man₅-Man₈ glycans were statistically elevated in the soluble cytosolic glycoproteins isolated from invasive and noninvasive breast cancer cells compared with those isolated from normal epithelial cells (32). Another report (33) shows high mannose oligosaccharides to be more prevalent in the cell surface of tumor cells compared with normal cells. It was suggested that tumor cells display high-mannose glycans because of the failure to undergo further glycosylation of the tumor cell surface in the Golgi.

N-linked glycans are synthesized first in the endoplasmic reticulum and later refined in the Golgi by competing glycosyl transferases (8). In glycan biosynthesis, the high-mannose

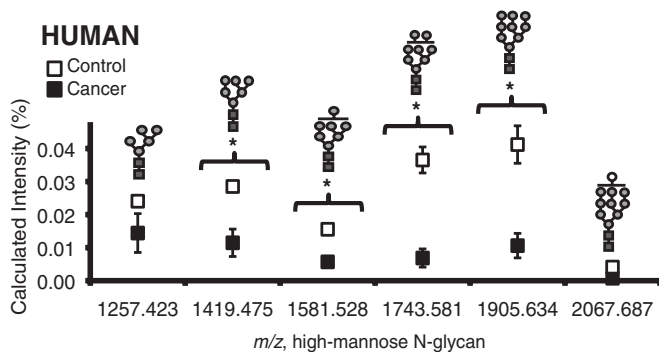


FIG. 6. High-mannose glycans in human sera of control ($n = 5$) and cancer ($n = 7$) groups. Glycans marked with * have p value < 0.05 . Glycans were analyzed using the internal standard method by MALDI FT-ICR MS. Error bars are expressed as S.E. See Fig. 1 for glycan symbols.

types are synthesized early in the process. High-mannose glycans play an important role in protein folding (34). They protect the proteins against degradation during intracellular transport (34–36). The mannose residues of the N -glycans are then cleaved sequentially and are replaced by N -acetylglucosamine and glucose residues to form complex and hybrid glycans. Most of the mature glycoproteins exiting the Golgi have complex N -glycans, whereas most of the glycoproteins found in the ER still carry the high-mannose glycans (37, 38). Because the secretory pathway involves both the ER and the Golgi, high mannose oligosaccharides are not abundant in serum profiles (25).

The elevation in intensities of high-mannose glycans suggests a premature termination of the glycosylation pathway and a problem during the synthesis that prohibits the deletion and subsequent addition of sugar residues. Indeed, mechanistic deviations in the earlier part of a biosynthetic pathway is known to limit the amounts of specific structural types and cause an increase in the amount of other structures (9). The increased presence of high mannose glycans, *vis-à-vis* complex or hybrid-type structures, has consequences for the function of the protein. It may, among other things, alter the stability of the protein, its ability to interact with other substrates, vary its half-life in blood and alter adhesion and communication properties of the protein.

Although this study requires further testing and validation, it suggests that the elevation of the high-mannose glycans may be a common theme in breast cancer. A bigger study involving more mouse and human samples is warranted given the positive results presented in this small-set study. Our ongoing studies for the human cancer biomarker discovery are in part targeted toward specific types of glycans, and we use other enzymes such as Endoglycosidase-H, a glycosidase that specifically cleaves N -linked mannose-rich glycans, to look more closely at the often-overlooked low-abundant high-mannose glycans.

Analysis of serum glycans by mass spectrometry represents a new paradigm in cancer biomarker studies, *i.e.* a

focus on post-translational modifications of proteins rather than protein expression. Changes in glycosylation during progression of the disease appear to be characteristic of the disease. To our knowledge, only a handful of papers correlate high-mannose glycans to breast cancer, or cancer in general. A trend in elevation both in the mouse and human sera, though requiring further validation, suggests that such a class of N -glycans may be altered in the presence of breast cancer.

* This work was supported in part by the National Institutes of Health (R01GM049077 to CBL) and Susan Komen (to HKC).

§ This article contains Supplemental Tables 1–3.

‡‡ To whom correspondence should be addressed: Department of Chemistry, University of California Davis, One Shields Avenue, Davis, CA 95616, Tel.: (530) 752-6364; Fax: (530) 752-8995; E-mail: cblebrilla@ucdavis.edu.

REFERENCES

- Garcia, M. J. A., *et al.* (2007) *Global Cancer Facts and Figures 2007*. American Cancer Society, Atlanta, GA
- Jemal, A., Siegel, R., Xu, J., and Ward, E. (2010) Cancer Statistics, 2010. *CA Cancer J. Clin.* **60**, 277–300
- Harris, L., *et al.* (2007) American society of clinical oncology 2007 update of recommendations for the use of tumor markers in breast cancer. *J. Clin. Oncol.* **25**, 5287–5312
- Safi, F., Kohler, I., Röttinger, E. and Beger, H. (1991) The value of the tumor marker CA 25–3 in diagnosing and monitoring breast cancer: A comparative study with carcinoembryonic antigen. *Cancer* **68**, 574–582
- Seregini, E., Coli, A., and Mazzucca, N. (2004) Circulating tumour markers in breast cancer. *Eur. J. Nucl. Med. Mol. Imaging* **31**, 515–522
- Stearns, V., Yamauchi, H., and Hayes, D. F. (1998) Circulating tumor markers in breast cancer: Accepted utilities and novel prospects. *Breast Cancer Res. Trends* **52**, 239–259
- Guadagni, F., *et al.* (2001) A re-evaluation of carcinoembryonic antigen (CEA) as a serum marker for breast cancer: A prospective longitudinal study. *Clin. Cancer Res.* **7**, 2357–2362
- Brooks, S. A., Dwek, M. V. and Schumacher, U. (2002) *Functional and molecular glycobiology*, BIOS Scientific Publishers Ltd, Oxford, UK
- Varki, A., *et al.* (2009) *Essentials of glycobiology*, 2nd Ed. Cold Spring Harbor Laboratory Press, New York
- Abd, Hamid, U. M., *et al.* (2008) A strategy to reveal potential glycan markers from serum glycoproteins associated with breast cancer progression. *Glycobiology* **18**, 1105–1118
- Kyselova, Z., *et al.* (2008) Breast cancer diagnosis and prognosis through quantitative measurements of serum glycan profiles. *Clin. Chem.* **54**, 1166–1175
- Alley, W. R., Madera, M., Mechref, Y., and Novotny, M. V. (2010) Chip-based reversed-phase liquid chromatography-mass spectrometry of permethylated N-linked glycans: A potential methodology for cancer-biomarker discovery. *Anal. Chem.* **82**, 5095–5106
- An, H. J., Kronewitter, S. R., de, Leoz, M. L., and Lebrilla, C. B. (2009) Glycomics and disease markers. *Current Opinion Chem. Biol.* **13**, 601–607
- Kirmiz, C., *et al.* (2007) A serum glycomics approach to breast cancer biomarkers. *Mol. Cellular Proteomics* **6**, 43–55
- Maglione, J. E., *et al.* (2001) Transgenic Polyoma middle-T mice model premalignant mammary disease. *Cancer Res.* **61**, 8298–8305
- Maglione, J. E., *et al.* (2004) Polyomavirus middle T-induced mammary intraepithelial neoplasia outgrowths: Single origin, divergent evolution, and multiple outcomes. *Mol. Cancer Ther.* **3**, 941–953
- Jessen, K. A., *et al.* (2004) Molecular analysis of metastasis in a polyomavirus middle T mouse model: the role of osteopontin. *Breast Cancer Res.* **6**, R157–R169
- de, Leoz, M. L., *et al.* (2008) Glycomics approach for potential biomarkers on prostate cancer: Profiling of N-linked glycans in human sera and pRNS cell lines. *Disease Markers* **25**, 243–258
- Kronewitter, S. R., *et al.* (2010) Human serum processing and analysis methods for rapid and reproducible N-glycan mass profiling. *J. Pro-*

- teome Res.* **9**, 4952–4959
20. An, H. J., *et al.* (2006) Profiling of glycans in serum for the discovery of potential biomarkers for ovarian cancer. *J. Proteome Res.* **5**, 1626–1635
 21. Kyselova, Z., *et al.* (2007) Alterations in the serum glycome due to metastatic prostate cancer. *J. Proteome Res.* **6**, 1822–1832
 22. Kita, Y., *et al.* (2007) Quantitative glycomics of human whole serum glycoproteins based on the standardized protocol for liberating N-glycans. *Mol. Cell. Proteomics* **6**, 1437–1445
 23. Morelle, W., *et al.* (2006) Mass spectrometric approach for screening modifications of total serum N-glycome in human diseases: application to cirrhosis. *Glycobiology* **16**, 281–293
 24. Kam, R. K., *et al.* (2007) High-throughput quantitative profiling of serum N-glycome by MALDI-TOF mass spectrometry and N-glycomic fingerprint of liver fibrosis. *Clin. Chem.* **53**, 1254–1263
 25. Kronewitter, S. R., *et al.* (2009) The development of retrosynthetic glycan libraries to profile and classify the human serum N-linked glycome. *Proteomics* **9**, 2986–2994
 26. Chu, C. S., *et al.* (2009) Profile of native N-linked glycan structures from human serum using high performance liquid chromatography on a microfluidic chip and time-of-flight mass spectrometry. *Proteomics* **9**, 1939–1951
 27. An, H. J., Tillinghast, J. S., Woodruff, D. L., Rocke, D. M., and Lebrilla, C. B. (2006) A new computer program (GlycoX) to determine simultaneously the glycosylation sites and oligosaccharide heterogeneity of glycoproteins. *J. Proteome Res.* **5**, 2800–2808
 28. Van, Oss, C. J. (1989) On the Mechanism of the Cold Ethanol Precipitation Method of Plasma-Protein Fractionation. *J. Protein Chem.* **8**, 661–668
 29. Lattova, E., Varman, S., Bezabeh, T., Petrus, L., and Perrault, H. (2008) Mass spectrometric profiling of N-linked oligosaccharides and uncommon glycoform in mouse serum with head and neck tumor. *J. Am. Soc. Mass Spectr.* **19**, 671–685
 30. Vanhooren, V., *et al.* (2007) N-glycomic changes in serum proteins during human aging. *Rejuvenation Res.* **10**, 521–531
 31. Vanhooren, V., Laroy, W., Libert, C., and Chen, C. (2008) N-Glycan profiling in the study of human aging. *Biogerontology* **9**, 351–356
 32. Goetz, J. A., Mechref, Y., Kang, P., Jeng, M. H., and Novotny, M. V. (2009) Glycomic profiling of invasive and non-invasive breast cancer cells. *Glycoconjugate J.* **26**, 117–131
 33. Johns, T. G., *et al.* (2005) The antitumor monoclonal antibody 806 recognizes a high-mannose form of the EGF receptor that reaches the cell surface when cells over-express the receptor. *FASEB J.* **19**(3):780–782
 34. Yamaguchi, H., and Uchida, M. (1996) A chaperone-like function of intramolecular high-mannose chains in the oxidative refolding of bovine pancreatic RNase B. *J. Biochem.* **120**, 474–477
 35. Morishima, S., *et al.* (2003) Expression and role of mannose receptor/terminal high-mannose type oligosaccharide on osteoclast precursors during osteoclast formation. *J. Endocrinol.* **176**, 285–292
 36. Driouch, A., Gonnet, P., Makkie, M., Laine, A.-c, and Faye, L. (1989) The role of high-mannose and complex asparagine-linked glycans in the secretion and stability of glycoproteins. *Planta* **180**, 96–104
 37. Vagin, O., Kraut, J. A., and Sachs, G. (2009) Role of N-glycosylation in trafficking of apical membrane proteins in epithelia. *Am. J. Physiol. Renal Physiol.* **296**, 459–469
 38. Helenius, A., and Aebi, M. (2001) Intracellular functions of N-linked glycans. *Science* **291**, 2364–2369
 39. Varki, A., *et al.* (2009) Symbol nomenclature for glycan representation. *Proteomics* **9**, 5398–5399